J Mater Sci: Mater Med (2015) 26:183
DOI 10.1007/s10856-015-5511-6

Structural and phase characterization of bioceramics prepared from tetracalcium phosphate–monetite cement and in vitro osteoblast response

Radoslava Stulajterova[1] · Lubomir Medvecky[1] · Maria Giretova[1] · Tibor Sopcak[1]

Received: 1 August 2014 / Accepted: 30 March 2015 / Published online: 17 April 2015

Abstract Biphasic porous calcium phosphate ceramics was prepared by sintering of transformed tetracalcium phosphate–monetite cement. After annealing hydroxyapatite, β- or α-TCP were found as main phases in ceramic substrates and a highly microporous microstructure of cement ceramics was created without an addition of porosifier. The origin microstructure features characteristic by the presence of hollow particle agglomerates in cement were preserved in microstructure of cement ceramics after annealing but the hydroxyapatite particles rose in size up to 2 μm and obtained a more regular shape. A small decrease in compressive strength was demonstrated in ceramics sintered up to 1150 °C and enhanced osteoblast proliferation was revealed on cement ceramic substrates in comparison with cement sample and conventional ceramics. The ALP activity of osteoblasts decreased with rise in sintering temperature. The prepared cement microporous ceramics could be utilized as carrier for antibiotics, drugs, growth factors, enzymes or other substances stimulating healing process.

1 Introduction

The calcium phosphate ceramics (CPCs) have been widely used for bone tissue repair and augmentation. They possess some bioactive surface properties that support the osteoblast adhesion/proliferation (i.e. osteoconduction) and stimulate the new bone formation (i.e. osteoinduction) [1]. Nonporous hydroxyapatite (HA) ceramics is a good example of a bioactive material, while porous bioceramic, which can consist of two-phase calcium orthophosphates (i.e., composites β-TCP (tricalcium phosphate) + HA or α-TCP + HA), is an example of a bioresorbable material. In the production of bioceramic, the calcination and fritting stages are very important [2]. The thermal stability of the synthetic HA depends on the Ca/P ratio and it decomposes even at 700 °C when the ratio is a lower than stoichiometric [3]. On the other hand, the thermal transformation of Ca-deficient hydroxyapatite (CDHA) to β-TCP [4] occurred within the temperature region 700–800 °C and heating at about 1160 °C caused the formation of the α-TCP. The proportion of HAP and TCP in the biphasic calcium phosphate mixtures after decomposition of the initial CDHA may also greatly influence sintering and the final microstructure of ceramics [5]. The calcium phosphate (CaP) ceramics was used to synthesize of bone-like scaffolds [6]. Andriotis et al. [7] reported a method for preparing CPCs by the calcination of CaP cements (based on hydrolysis of the α-TCP) composed mainly of calcium deficient hydroxyapatite (CDHA). Miao et al. [8] prepared the sintered porous CPCs by coating polyurethane foams with a CaP cement (on tetracalcium phosphate (TTCP) basis) followed by annealing at 1200 °C. A larger number of osteoblast-like cells was found to be attached to the etched and rough osteoceramic surfaces [9]. Cell adhesion, proliferation and detachment strength increased and both the short- and longer-term response of bone marrow cells in vitro were improved with the roughness of HA [10]. It has been suggested that the crystallite size of HA may play an important role in governing the expression of osteoblast activities [11]. The granular HA and α- and β-tricalcium phosphate supported, whereas nanosized HA inhibited viability of osteoblast cells [12]. Ball et al. [13] reported

✉ Lubomir Medvecky
lmedvecky@imr.saske.sk

[1] Institute of Materials Research of SAS, Watsonova 47, 04001 Kosice, Slovakia

that the cell responses to the surfaces were influenced primarily by the topography of the surfaces.

In this work, we studied the possibility of the preparation of porous CPC (HA ceramic) from the tetracalcium phosphate–nanomonetite biocement without porosifier addition. Advantage of this preparation method could be obtaining variously shaped ceramic substrates from the origin simple cement paste and the formation of the biphasic CPCs composed of β- or α-TCP +HA without the presence of β,α-TCP phase mixture in HA ceramics commonly formed during sintering of the nanohydroxyapatite synthesized by the conventional method (e.g. precipitation). The development of microstructure, analysis of the phase composition and in vitro cytotoxicity of the final ceramics were evaluated in the paper.

2 Materials and methods

2.1 Preparation of powder mixture and HA conventional ceramic discs

Tetracalcium phosphate ($Ca_4(PO_4)_2O$, TTCP) was prepared by annealing an equimolar mixture of calcium carbonate ($CaCO_3$, analytical grade, Sigma-Aldrich) and dicalcium phosphate anhydrous (DCPA) ($CaHPO_4$ (Ph. Eur.), Fluka), at 1450 °C for 5 h. After cooling, the product was crushed by milling in a planetary ball mill (Fritsch) for 2 h and the phase purity was evaluated using the X-ray powder diffraction analysis (XRD, Philips X Pert Pro). The powder cement mixture was synthesized by in situ reaction between TTCP and diluted solution of the orthophosphoric acid (analytical grade, Merck) in ethanol (1:4). The ethanolic orthophosphoric acid solution/TTCP ratio was 1. The H_3PO_4 was added at such an amount that the final Ca/P mole ratio in powder mixture was equal to 1.67, which corresponds to the Ca/P mole ratio in HA.

HA for the preparation of conventional ceramics was synthesized by the co-precipitation of 0.5 M $Ca(NO_3)_2$ (analytical grade) and 0.5 M $(NH_4)_2HPO_4$ (analytical grade) solutions (molar ratio of Ca/P = 1.67). The aqueous solution of $Ca(NO_3)_2$ was slowly dropped to $(NH_4)_2HPO_4$ aqueous solution for 1.5 h. The pH at the end of the precipitation was adjusted and kept at 10.5 by adding NH_3(aq) (1:1). The rotation speed of stirrer was 450 rpm and the precipitation was done at 25 °C. Ageing time was 72 h. Precipitates were washed with distilled water, filtered over the membrane filter (Millipore, 0.2 μm pore size) and dried at 110 °C for 4 h. The dry powders were crushed, sieved (Mesh 250), pressed under 70 MPa into the pellet form (6 mm D × 12 mm H for measurement of compressive strength and 6 mm D × 0.5 mm H for in vitro testing) and sintered at 1150 °C for 1 h. This sample was prepared for the comparison of its properties with the ceramics made from cement at the same temperature.

2.2 Characterization methods and preparation of cement ceramics

The 2 % NaH_2PO_4 (analytical grade, Sigma-Aldrich) solution was used as a hardening liquid. The P/L ratio was 2. The cement paste was moulded into the pellet form (6 mm D × 12 mm H for measurement of compressive strength and 6 mm D × 0.5 mm H for in vitro testing) by packing in stainless cylindrical form. Samples were hardened in PBS solution at 37 °C for 24 h and dried at 80 °C for 2 h. Cement ceramics was prepared by sintering of hardened cement samples at 1050, 1150 and 1300 °C for 1 h. The heating rate was kept at 10 °C/h and cooling rate was given by naturally cooling of the furnace in the case of cement ceramics sintered at 1050, 1150 °C. The ceramics annealed at 1300 °C was rapidly cooled for preserving the formation of α-TCP.

The compressive strength (mean of 3 samples) of samples was measured on a universal testing machine (LR5K Plus, Lloyd Instruments Ltd.) at crosshead speeds of 1 mm/min.

The phase compositions of samples were analyzed by the XRD analysis (Philips X' PertPro, using Cu Kα radiation). The microstructures of fractured surfaces of samples after 24 h were observed by the field emission scanning electron microscopy (JEOL FE SEM JSM-7000F). Densities of samples were calculated from their weights and dimensions.

2.3 Cell cultivation and viability testing

MC3T3E1 preosteoblastic murine cells were purchased from ECAAC, Salisbury, UK. The cells were removed from culture flasks by enzymatic digestion and then resuspended in culture medium and the cell suspension was adjusted at a density of 10^5 cells/mL.

Ceramic scaffolds were sterilized in an autoclave at 121 °C. The sterilized scaffolds were placed in wells of 96-well suspension plate. Complete culture α-modification minimum essential Eagle medium (αMEM) with 10 % Fetal bovine serum, 1 % ATB–ATM and osteogenic supplements: β-glycerophosphate 10 mM, ascorbic acid 50 μg/mL and dexametasone 50 nM (Sigma-Aldrich) in amount of 200 μL with 2.0×10^4 MC3T3E1 cells were carefully added to surfaces of each disc in wells. All experiments were performed fourfold for each sample. As negative controls were considered cells in wells cultured without tested TTCP discs by above described culture conditions in wells of 96-well tissue culture treated plate (cellGrade, Brand). The cells were cultured at 37 °C, 95 %

humidity and 5 % CO_2 in incubator. Cells were allowed to adhere and after 24 h adherence, the complete culture media were replaced. The complete culture medium was changed every 2 days.

After 2 and 8 days of culturing, the proliferation of the cells, ALP activity, DNA content and fluorescent images of cells on samples were determined. The proliferation was evaluated by a commercially purchased in vitro toxicology assay kit (In-vitro toxicology assay kit, resazurin based; Sigma-Aldrich) according to the manufacturer's instructions for use. The absorbance of final product (resorufin) was determined after 3 h of cell culture at 600 nm by UV Vis spectrophotometer. The measured absorbances of medium from wells with cell seeded on substrates were compared with absorbances of medium from wells with cells free of substrates and cultured for 8 days in the tissue culture polystyrene plate (control, treated 96-well tissue culture plate, Santa Cruz Biotechnology, Santa Cruz, USA). The pure complete culture medium was used as a blank.

The ALP activity of osteoblasts was determined using the phosphatase substrate (Sigma-Aldrich, 5 mg tablet in 5 mL diethanolamine buffer, pH = 9.8). Attached osteoblasts were lysed by adding 200 μL phosphate buffer saline with 0.1 % (v/v) of Triton X-100, 20 mM Tris and 1 mM $MgCl_2$ to each well, followed by freezing at −20 °C for 1 h and centrifuged at 10,000 rpm for 10 min. The 100 μL phosphatase substrate was added to 100 μL of cell lysate and the mixture was incubated at 37 °C for 1 h. The alkaline phosphatase reaction was stopped by the addition of 50 μL of 3 M NaOH. The concentration of p-nitrophenol was determined from a calibration curve using UV Vis spectrophotometry at 405 nm. The ALP activity were expressed in μmoles of p-nitrophenol produced per 1 min/μg of DNA. The statistical evaluation of results (n = 3) was performed using ANOVA analysis at level $\alpha = 0.05$.

The DNA content in samples or control wells after cultivation was evaluated by the fluorescence method (fluorometer Picofluor, Turner Biosystems) with the Hoechst 33258 dye. The calf thymus DNA (Sigma-Aldrich) was used for calibration.

The density, distribution and morphology of the MC3T3E1 cells grown on tested discs were visualized with fluorescent live/dead staining (fluorescein diacetate/propidium iodide) by an inverted optical fluorescence microscope (Leica DM IL LED, blue filter).

3 Results and discussion

3.1 XRD analysis of materials

The XRD analysis (Fig. 1) showed changes in the phase composition of cement after annealing at various temperatures. The hardened cement was composed of calcium deficient nanocrystalline HA, which was partially decomposed to crystalline HA (JCPDS 72-1243) and β-TCP (JCPDS 09-0169) after sintering at 1050 °C. No changes in the phase composition and content of β-TCP were observed after heating at temperature of 1150 °C what is in accordance with the $CaO–P_2O_5$ phase diagram. The further increase in temperature to 1300 °C caused the phase transformation of β-TCP to α-TCP (JCPDS 29-0359), which was stabilized by a fast cooling of ceramics. Note that this procedure was used especially for preserving of the α-TCP in final ceramics because this component could be improve the bioactivity of substrate.

In the case of conventional HA ceramics, both the β-TCP and α-TCP minor phases were found in HA ceramics after sintering at 1150 °C and the mean contents of βTCP and αTCP in ceramics were 17 ± 12 and 14 ± 7 wt% respectively (determined by the Rietveld analysis of XRD patterns).

3.2 Morphology and size of calcium phosphate particles in hardened cement and sintered ceramics

The morphology and size of CaP particles in hardened cement and ceramic samples are shown in Fig. 2. In the microstructure of origin CaP cement after 24 h hardening in PBS solution (Fig. 2a), the agglomerated needle-like fine HA particles with length <500 nm and diameter between 60 and 80 nm are clearly visible. The rounded hollow agglomerates of nanohydroxyapatite particles are characteristic by coarse wall around circle or elliptically shaped hole (about 1–5 μm size) located in the center of agglomerate. Besides the irregularly shaped pores (1–2 μm size) were observed in microstructure between agglomerates. This agglomerate morphology originated from dissolution/precipitation processes based on dissolution of the individual CaP components in powder cement mixture—TTCP and monetite particles—and following precipitation of nanohydroxyapatite particles. After cement sintering at 1050 °C/1 h (Fig. 2b) the morphology of origin needle-like HAP particles was fully changed and HA particles obtained the spherical shape with clearly visible necks characteristic for interconnection between individual particles as the result of sintering. The particles with smooth surfaces had average size of 0.5 μm. A large amount of the small irregularly shaped pores (with dimensions up to 500 nm) can be observed between particles in a low dense microstructure of ceramics. The special ellipse-like hollow objects were found in the cement ceramics with the size around 3–5 μm, which copy the morphology of similar agglomerates in origin cement. The cavity in core of objects is surrounded by the dense HA shell, which is created from nanohydroxyapatite particles

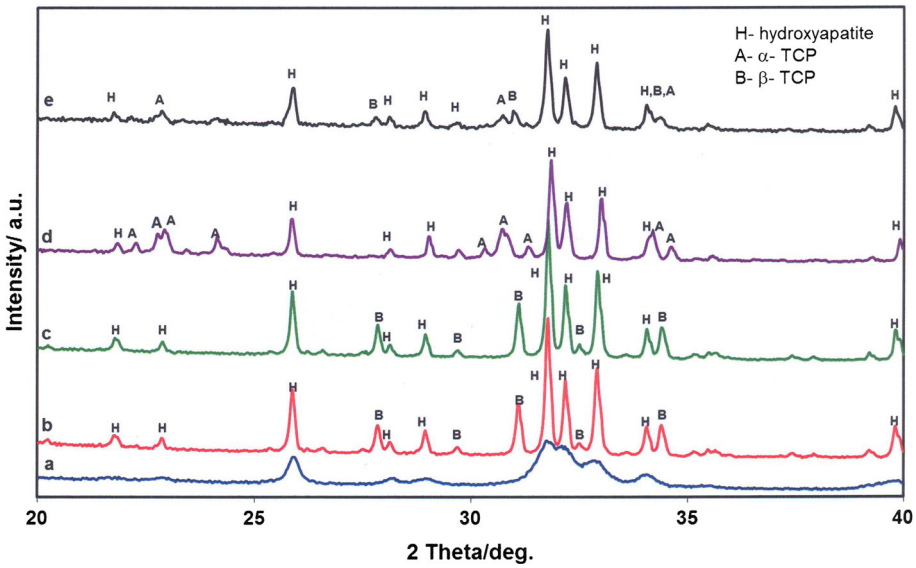

Fig. 1 XRD patterns of hardened cement (*a*) and ceramic substrates after sintering at 1050 °C (*b*), 1150 °C (*c*), 1300 °C (*d*) and conventional ceramics (*e*) sintered at 1150 °C for 1 h

localized in walls of hollow cement agglomerates. Coarsening of the HA particles was observed during sintering of cement at 1150 °C (Fig. 2c). The grain size rose approximately twice up to 1 μm and grains had spherical morphology with a tightly interconnection after sintering. Nanopores found in the microstructure of cement ceramics annealed at lower temperatures were enlarged by coalescence and achieved about 2 μm size. Note that the microstructure had sponge-like character with a high fraction of open pores allows the exchange of ions and nutrients from environment. The characteristic ellipse-like hollow objects were still visible in microstructure. After annealing at 1300 °C, irregularly shaped large (~2 μm in size) and spherical micropores were observed in the microstructure of ceramics (Fig. 2d). Note that the origin microstructure features characteristic for hollow particle agglomerates were preserved by annealing but the HA particles rose in size up to 2 μm and obtained a more regular shape.

The transgranular fracture mode is clearly visible in microstructure of conventional ceramics (Fig. 2e) and the average grain size was approximately 1 μm. Irregular small pores, found in scaffolds, do not exceed micrometer dimension. Grains had a characteristic angular shape, which corresponds with the hexagonal crystallographic symmetry of HA. Microstructure was significantly denser (around 15 vol% of the porosity) than this one of the cement ceramics sintered at 1150 °C, which reduces diffusion of any chemical substances over ceramics (e.g. nutrients from medium).

3.3 Influence of sintering temperature on the compressive strength and porosity of ceramics

The influence of sintering temperature or density on the compressive strength (CS) of ceramics is shown in Table 1. From comparison resulted that the compressive strength of hardened cement was 24 MPa and a small decrease in CS (to about 20 MPa) after annealing of cement at 1050 or 1150 °C was found irregardless the rise in density of samples. The reason of this fact could be the formation of a high amount of micropores in ceramic microstructure despite of joins in necks between individual particles. Besides, the mutual interconnections of agglomerates via needle-like nanoparticles at agglomerate boundaries were fully destroyed after sintering. No statistically significant differences were observed between CS of these ceramic samples. On the other hand, around 50 % increase of CS was found in cement ceramics sintered at 1300 °C, which corresponds with its more dense microstructure. Similar decrease of porosity led to the increase of compressive strength in work of Liu [14], where the microporous HA ceramics exhibited higher CS (20–30 MPa) than macroporous and the volume open porosity achieved 45–60 vol%. Mostafa [15] compared CS and densification processes of HA ceramics prepared from morphologically different HA particles. It was demonstrated that the larger calcium deficient needle-like HA particles start sintering at lower temperature (1000 °C) than the stoichiometric spherical nanosized HA due to faster diffusion ions in crystal lattice. Besides, a very similar microstructure in ceramics with open porosity like in our samples was found at 1000 °C. The CS of ceramics with 50 vol% porosity was about 20 MPa. Swain and Bhattacharyya [16] fabricated macroporous pure HA ceramics with 35 vol% porosity and CS equal 10 MPa at sintering temperature of 1250 °C but the average pore size was about 125 μm, which was much higher pore size than in our ceramics. The prepared conventional ceramics had almost half porosity in comparison with cement ceramics annealed at 1150 °C and

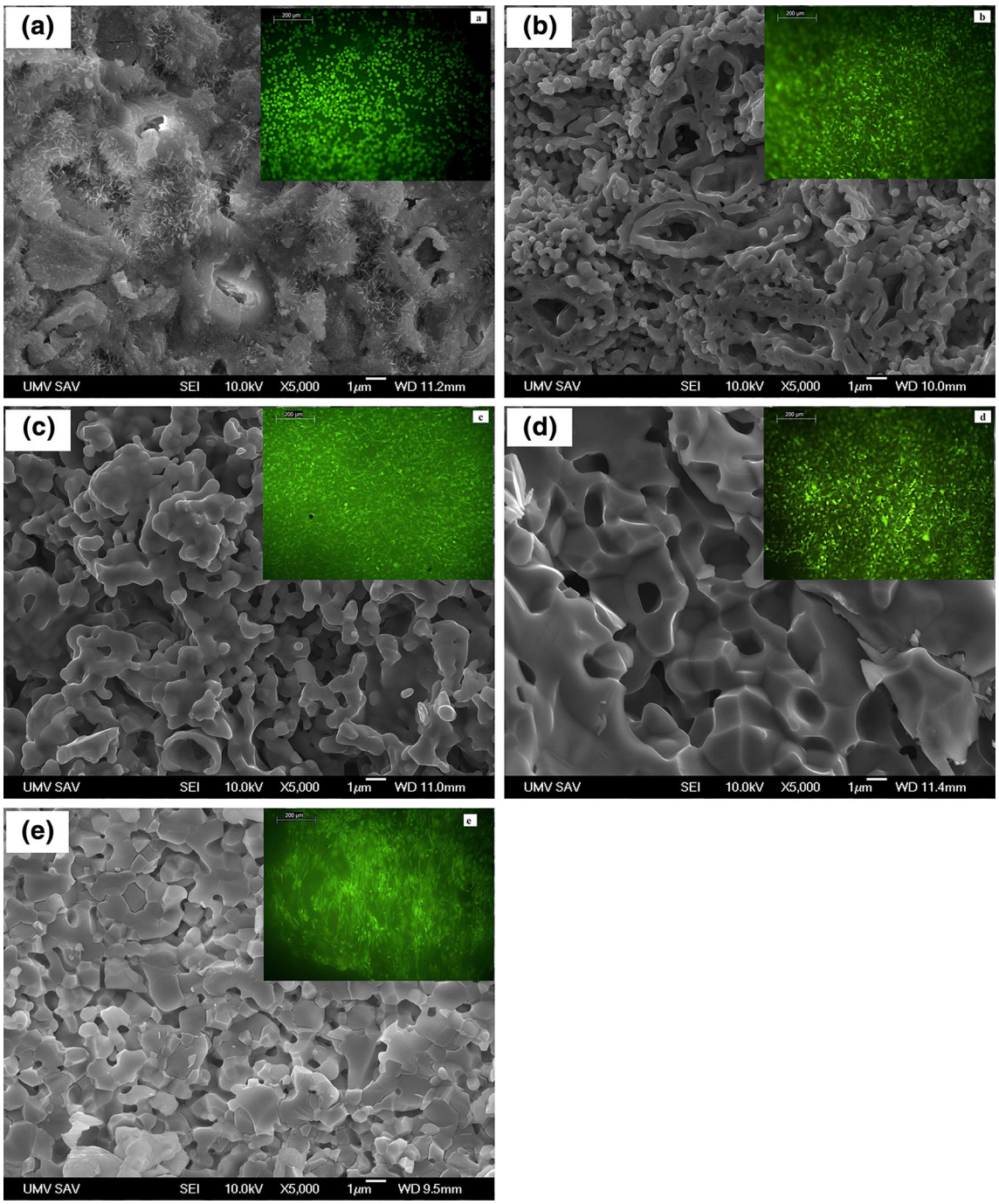

Fig. 2 Microstructures and distribution of osteoblasts on surfaces of substrates after 8 days of proliferation at 37 °C, 5 % CO_2 and 95 % humidity observed by the fluorescent optical microscopy (live/dead staining) (hardened cement (**a**), ceramics sintered at 1050 °C (**b**), 1150 °C (**c**), 1300 °C (**d**) and conventional ceramics (**e**) sintered at 1150 °C for 1 h)

this fact together with a more regularly shaped grains in ceramics were the main reason for the rise in its CS to 340 MPa. It has been reported [17] that the compressive strength of material with similar composition (73 wt% of HA and 27 wt% of β-TCP) as in our study but with a lower porosity (3–6 %) was around 544 MPa.

3.4 The structural changes of calcium phosphate ceramics during sintering process

It is known that the partial decomposition of CDHA to β-, α-TCP or βα-TCP mixture occurs in CPCs [18] in dependence on applied temperature (transformation temperature

Table 1 Sintering temperatures, phase composition, compressive strength and porosity of substrates

Sintering temperature (°C)	XRD analysis	Compressive strength (MPa)
Cement	nanoHAP	24 ± 3.79
1050	HAP, β-TCP	20 ± 2.08
1150	HAP, β-TCP	22 ± 4.36
1300	HAP, α-TCP	36 ± 1.53
Ceramics 1150	HAP, α,β-TCP	340 ± 50

around 1200 °C). Raynaud et al. [5] observed that the volume expansion accompanying the allotropic transformation of the TCP phase was not noticeable in HAP/TCP ceramics containing a lower amount of TCP (<30 wt%). Besides the biphasic ceramics had the lower sinterability in comparison with the stoichiometric HAP. The allotropic transformation of β-TCP to α-TCP was described by Nakamura et al. [19] who sintered hydroxyapatite-β-tricalcium phosphate mixture and showed a sharp thermal expansion above 1180 °C due to α-phase formation. In the case of our system, we assume that this effect did not strongly influence the microstructure formation of the cement ceramics sintered at lower temperatures (under transformation temperatures and with the high porosity) but because of approximately 30 % content of TCP, the higher strain and rapid cooling of the sample can be the reason for the presence of cracks in several ceramic samples with dimensions for the compressive strength evaluation sintered at 1300 °C. Note that these samples were excluded from testing.

3.5 Proliferation and ALP activity of osteoblasts on surface of substrates

Micrographs from the optical fluorescent microscope and SEM (Figs. 2, 3) show the morphology and density of osteoblasts proliferated on surface of substrates for 8 days. The lowest number of osteoblasts with well-spreaded cells and shorter filopodia between cells was found on cement substrate (Fig. 3a). Beside the regions free of osteoblast were clearly visible on sample surface (Fig. 2a). No similar areas were observed on ceramic samples. In comparison with the cement substrate, osteoblasts on cement ceramics samples had a more prolonged shape with the long filopodia interconnecting adjacent cells (Fig. 3b, c). A high cell density was revealed on cement ceramics sintered at 1300 °C with multilayered cell coating (Figs. 2d, 3d). A more prolonged morphology of osteoblasts was found on conventional ceramics (Figs. 2e, 3e) but it is clearly visible from Fig. 3c, e that the surface of conventional ceramics was smoother than its analogue prepared from cement, which corresponds with a denser microstructure of the sample. The gradual growth in cell population with sintering temperature was verified by the Alamar blue test in Fig. 4a, where the proliferation of osteoblasts on substrates rose with annealing temperature. This dependence was better observable in proliferation test of osteoblasts cultured on substrates for 8 days. Almost 100 % cell proliferation related to the negative control (resorufin absorbance in wells without substrate and cultured for 8 days) was found on ceramics sintered at 1300 °C. In the case of other ceramic samples, the cell proliferations were above the 70 % of the proliferation activity of osteoblasts in negative control that represents the limit for the potentially cytotoxic behaviour of biomaterials. A lower proliferation activity of osteoblasts was found on the cement sample, which was probably caused by the extremely fine needle-like HA particles in cement microstructure. From the comparison of the proliferation activity of osteoblasts cultured on cement ceramics and conventional ceramics resulted that the growth of osteoblast population was about 30 % higher on cement ceramic substrate. Shi et al. [20] showed a significant increase of the cell apoptosis of osteoblasts in contact with the thin rod-like HA particles. Wang et al. [21] revealed the improved cell proliferation on ceramic samples composed of crystalline HA particles with size around 1 μm and smoother surfaces. A lower osteoblast density was observed on HA substrates with the needle-like particles than on substrates composed of the spherical particles [22], which verified a low proliferation of osteoblasts on cement sample Woo et al. [23] showed the strong effect of the protein adsorption by HA surface on proliferation, differentiation and apoptosis of osteoblasts, where the higher pre-adsorbed amounts of extracellular matrix proteins or serum proteins supported the cell attachment and cell proliferation. On the other hand, the osteoblast adhesion, proliferation and detachment strength increased with the rise in roughness of HA ceramics [10]. These facts can be the reason for improving of the proliferation activity of osteoblasts cultured on cement ceramic substrate than on conventional ceramics because of a significantly higher porosity of this sample, which allows a much higher surface and pore volume for the adsorption of extracellular matrix proteins from serum. The cell proliferation, protein synthesis, ALP activity, and bone-like nodule favored surfaces with a more regular topography and lower microporosity [24] and our findings are in an

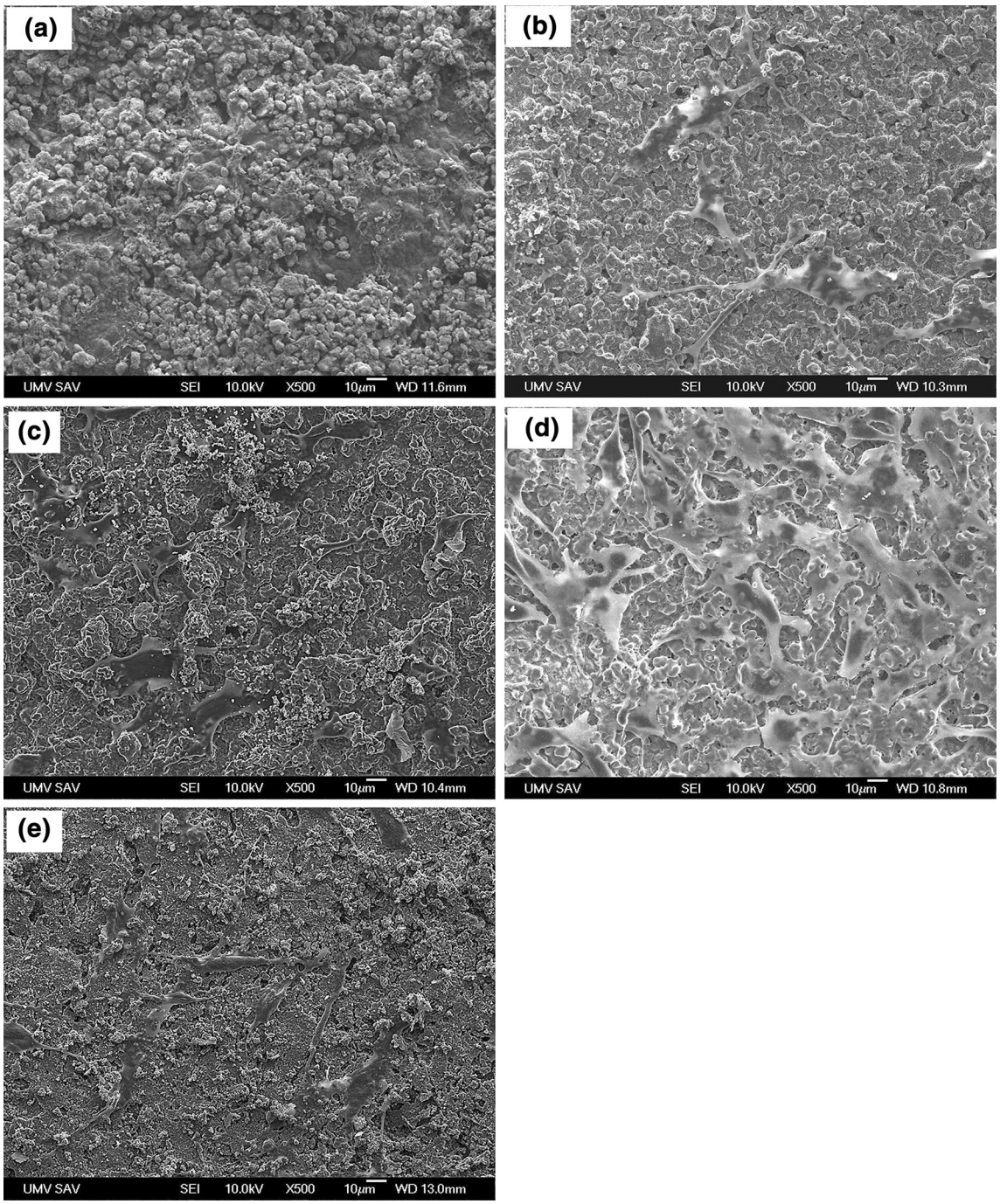

Fig. 3 Morphology of osteoblasts on substrates after 8 days of proliferation at 37 °C, 5 % CO_2 and 95 % humidity observed by the SEM (hardened cement (**a**), ceramics sintered at 1050 °C (**b**), 1150 °C (**c**), 1300 °C (**d**) and conventional ceramics (**e**) sintered at 1150 °C)

accordance with above results because the reduced microporosity was found in cement ceramics sintered at 1300 °C.

From the comparison of osteoblast ALP activity after 2 and 8 days of culture (Fig. 4b) resulted a high ALP activity of osteoblasts on cement surface, which was gradualy reduced in ceramics with the rise in annealing temperature. The CaP deposits are well visible in Fig. 3c, e in the form of extremely fine particles on cell surfaces. The rise in in vitro ALP activity of cells were found in macroporous scaffolds prepared from CPC [25]. He et al. [26] showed that the best ALP activity had substrates prepared from the nanohydroxyapatite than substrates consisted of microsized HA. It is clear that substrates contained the amorphous calcium phosphates or nanohydroxyapatite partially dissolve what causes the increase in calcium and phosphate

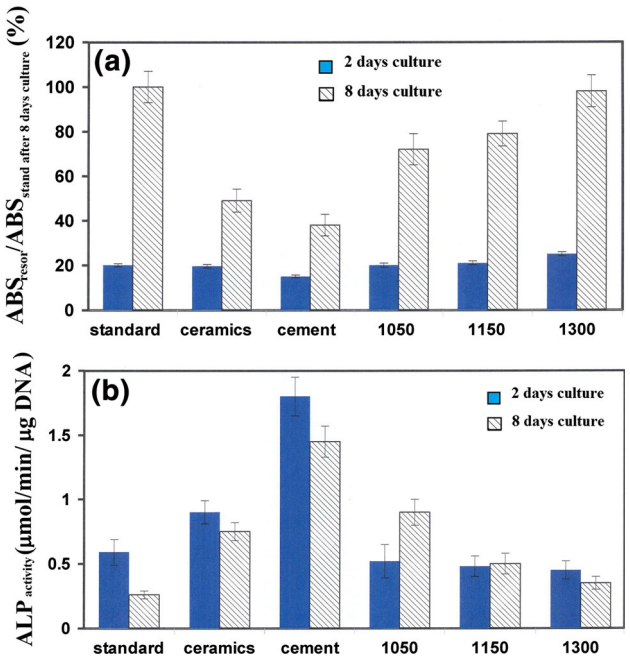

Fig. 4 Osteoblast proliferation on substrates measured by conversion of Alamar blue relatively to negative control (wells with cells cultured for 8 days) (**a**) and ALP activity of osteoblasts on substrates cultured for 2 and 8 days at 37 °C, 5 % CO_2 and 95 % humidity (**b**)

ions concentrations. Ogata et al. [27] verified the promotion of alkaline phosphatase activity, the expression of type I collagen, and bone-like tissue formation in extracts from more soluble CaP mixtures. Lin et al. [28] demonstrated about 30 % and even double rise in the solubility of threephasic α,βTCP-HA system in comparison with the pure α-TCP and biphasic βTCP-HA system respectively. Legeros et al. [29] showed the strong dependence of biphasic CPCs solubility on sintering conditions. Note that the presence of α-TCP in ceramics had the insignificant effect on the ALP activity probably due to a slow dissolution and following ion diffusion in direction out of sample. From the comparison of ALP activities of osteoblasts after 8 days of cultivation on cement ceramics resulted that the ALP osteoblast activity was almost double on substrate sintered at 1050 °C than on sample annealed at higher temperature and this fact supports above opinion. Besides both samples contained the same amount of β-TCP but the ceramics prepared at lower temperature had approximately half grain size found in cement ceramics annealed at 1150 °C, which again can enhance dissolution of phases in sample. On the other side, the improved ALP activity of osteoblasts was measured on the conventional ceramics, which was more dense but contained simultaneously α- and β-TCP. We believe that a much higher solubility of the threephasic system in conventional ceramics supported the ALP activity of osteoblasts cultured on the sample. Note that the dissolution behaviour of the biphasic CPCs is one of parameters (others e.g. topography, chemical character of the surface etc.) that affect the ALP activity of osteoblasts [30].

4 Conclusion

Biphasic porous CPCs with HA as the major and α- or β-TCP as the minor components was prepared by a novel method based on sintering of transformed CaP tetracalcium phosphate–nanomonetite cement. The gradual decrease in porosity and compressive strength was found with sintering temperature but after annealing up to 1150 °C, the density of samples rose only about 15 % from its origin value in cement because of the change in HA particle morphology and the porous microstructure formation during sintering. The cement ceramics had improved proliferation activity in comparison with conventional ceramics as the reason of enhanced roughness and a high fraction of micropores. The osteoblast proliferation was improved by cement annealing but the ALP activity decreased with sintering temperature probably as the result of the different dissolution rate of CaP phases in cement ceramics. It can be assumed that the cement ceramics could be show stronger osteoinductive and osteoconductive properties due to appropriate microtopography, possible higher adsorption of specific proteins, cytokines, growth factors and bone morphogenic proteins, which support the cell attachment and the differentiation of mesenchymal stem cells to osteoprogenitor cells after implantation into body. The prepared cement ceramics can be potentially applied as carriers for antibiotics, drugs, growth factors, enzymes or other substances stimulating healing process.

Acknowledgments This work was supported by the Slovak Grant Agency of the Ministry of Education of the Slovak Republic and the Slovak Academy of Sciences, Project No. 2/0047/14 and within the framework of the project "Advanced implants seeded with stem cells for hard tissues regeneration and reconstruction", which is supported by the Operational Program "Research and Development" financed through the European Regional Development Fund.

References

1. Samavedi S, Whittington AR, Goldstein AS. Calcium phosphate ceramics in bone tissue engineering: a review of properties and their influence on cell behavior. Acta Biomater. 2013;9:8037–45.
2. Dorozhkin SV. Bioceramics based on calcium orthophosphates. Glass Ceram. 2007;64(11–12):442–7.
3. Raynaud S, Champion E, Bernache-Assolant D, Thomas P. Calcium phosphate apatites with variable Ca/P atomic ratio I. Synthesis, characterization and thermal stability of powders. Biomaterials. 2002;23:1065–72.
4. Gibson IR, Rehman I, Best SM, Bonfield W. Characterization of the transformation from calcium deficient apatite to β-tricalcium phosphate. J Mater Sci Mater Med. 2000;12:799–804.

5. Raynaud S, Champion E, Bernache-Assolant D. Calcium phosphate apatites with variable Ca/P atomic ratio II. Calcination and sintering. Biomaterials. 2002;23:1073–80.
6. Oh S, Oh NJ, Appleford M, Ong JL. Bioceramics for tissue engineering applications—a review. Am J Biochem Biotechnol. 2006;2:49–56.
7. Andriotis O, Katsamenis OL, Mouzakis DE, Bouropoulos N. Preparation and characterization of bioceramics produced from calcium phosphate cements. Cryst Res Technol. 2010;45:239–43.
8. Miao X, Hu Y, Liu J, Wong AP. Porous calcium phosphate ceramics prepared by coating polyurethane foams with calcium phosphate cements. Mater Lett. 2004;58:397–402.
9. Keller JC, Collins JG, Niederauer GG, McGee TD. In vitro attachment of osteoblast-like cells to osteoceramic materials. Dent Mater. 1997;13:62–8.
10. Deligianni DD, Katsala ND, Koutsoukos PG, Missirlis YF. Effect of surface roughness of hydroxyapatite on human bone marrow cell adhesion, proliferation and detachment strength. Biomaterials. 2001;22:87–96.
11. Ong JL, Hoppe CA, Cardenas HL, Cavin R, Carnes DL, Sogal A, Raikar GN. Osteoblast precursor cell activity on HA surfaces of different treatments. J Biomed Mat Res Part A. 1998;39:176–83.
12. Herten M, Rothamel D, Schwarz F, Friesen K, Koegler G, Becker J. Surface-and nonsurface-dependent in vitro effects of bone substitutes on cell viability. Clin Oral Investig. 2009;13:149–55.
13. Ball M, Grant DM, Lo WJ, Schotchford CA. The effect of different surface morphology and roughness on osteoblast-like cells. J Biomed Mater Res Part A. 2008;86(3):637–47.
14. Liu DM. Influence of porosity and pore size on the compressive strength of porous hydroxyapatite ceramics. Ceram Int. 1997;23:135–9.
15. Mostafa NY. Characterization, thermal stability and sintering of hydroxyapatite powders prepared by different routes. Mater Chem Phys. 2005;94:333–41.
16. Swain SK, Bhattacharyya S. Preparation of high strength macroporous hydroxyapatite scaffold. Mater Sci Eng C. 2013;33:67–71.
17. Zyman ZZ, Tkachenko MV, Polevodin DV. Preparation and characterization of biphasic calcium phosphate ceramics of desired composition. J Mater Sci Mater Med. 2008;19:2819.
18. Kivrak N, Tas AC. Synthesis of calcium hydroxyapatite-tricalcium phosphate (HA-TCP) composite bioceramic powders and their sintering behavior. J Am Ceram Soc. 1998;81(9):2245–52.
19. Nakamura S, Otsuka R, Aoki H, Akao M, Miura N, Yamamoto T. Thermal expansion of hydroxyapatite-β-tricalcium phosphate ceramics. Thermochim Acta. 1990;165:57–72.
20. Shi Z, Huang X, Cai Y, Tang R, Yang D. Size effect of hydroxyapatite nanoparticles on proliferation and apoptosis of osteoblast-like cells. Acta Biomater. 2009;5:338–45.
21. Wang C, Duan Y, Markovic B, Barbara J, Rolfe Howlett C, Zhang X, Zreiqat H. Proliferation and bone-related gene expression of osteoblasts grown on hydroxyapatite ceramics sintered at different temperature. Biomaterials. 2004;25:2949–56.
22. Xu JL, Khor KA, Sui JJ, Zhang JH, Chen WN. Protein expression profiles in osteoblasts in response to differentially shaped hydroxyapatite nanoparticles. Biomaterials. 2009;30:5385–91.
23. Woo KM, Seo J, Zhang R, Ma PX. Suppression of apoptosis by enhanced protein adsorption on polymer/hydroxyapatite composite scaffolds. Biomaterials. 2007;28:2622–30.
24. Rosa AL, Beloti MM, van Noort R. Osteoblastic differentiation of cultured rat bone marrow cells on hydroxyapatite with different surface topography. Dent Mater. 2003;19:768–72.
25. Wang JC, Ko CL, Hung CC, Tyan YC, Lai CH, Chen WC, Wang CK. Deriving fast setting properties of tetracalcium phosphate/dicalcium phosphate anhydrous bone cement with nanocrystallites on the reactant surfaces. J Dent. 2010;38:158–65.
26. He HW, Li GD, Li B, Chen ZQ. Effects of surface microstructure of hydroxyapatite on protein adsorption and biological performance of osteoblasts. Appl Surf Sci. 2008;255:565–7.
27. Korenori O, Satoshi I, Atsushi E, Shigeyuki E, Yoshifumi K, Takayoshi N, Yukichi U. Comparison of osteoblast responses to hydroxyapatite and hydroxyapatite/soluble calcium phosphate composites. J Biomed Mater Res. 2005;72A:127–35.
28. Lin FH, Liao CJ, Chen KS, Sun JS, Lin CP. Petal-like apatite formed on the surface of tricalcium phosphate ceramic after soaking in distilled water. Biomaterials. 2001;22:2981–92.
29. Legeros RZ, Lin S, Rohanizadeh R, Mijares D, Legeros JP. Biphasic calcium phosphate bioceramics: preparation, properties and applications. J Mater Sci Mater Med. 2013;14:201–9.
30. Kong YM, Kim HE, Kim HW. Phase conversion of tricalcium phosphate into Ca-deficient apatite during sintering of hydroxyapatite–tricalcium phosphate biphasic ceramics. J Biomed Mater Res Part B. 2008;84B:334–9.